Downloaded from http://cshprotocols.cshlp.org/ at Yale University on November 6, 2015 - Published by Cold Spring Harbor Laboratory Press

Protocol

Voltage-Sensitive Dye Imaging of Population Signals in Brain Slices

Bradley Baker, Xin Gao, Brian S. Wolff, Lei Jin, Lawrence B. Cohen, Chun X. Bleau, and J.-Y. Wu

In a bright-field measurement from a vertebrate brain stained by superfusing a solution of the dye over the surface, each pixel in a camera receives light from a substantial number (thousands) of neurons and neuronal processes (population signals). Because of scattering and out-of-focus light, this will be true even if the pixel size corresponds to a small area of the brain. In this situation, the voltage-sensitive dye signal will be a population average of the change in membrane potential of all of these neurons and processes. Many investigators have published voltage-sensitive dye imaging studies of population activities in brain slices. Their methods, including choice of dyes, illumination intensity, and imaging device, vary across a large spectrum. Here we present a protocol for visualizing spatiotemporal patterns in rodent neocortex in vitro. Detecting these patterns requires high-sensitivity imaging in single trials, because averaging will obscure the complex dynamics of the spatiotemporal patterns.

Cold Spring Harbor Protocols | www.cshprotocols.org

MATERIALS

It is essential that you consult the appropriate Material Safety Data Sheets and your institution's Environmental Health and Safety Office for proper handling of equipment and hazardous material used in this protocol.

RECIPES: Please see the end of this protocol for recipes indicated by <R>. Additional recipes can be found online at http://cshprotocols.cshlp.org/site/recipes.

Reagents

Brain (rodent)
Holding artificial cerebrospinal fluid (ACSF) <R>
Modified ACSF (prechilled to 4°C) <R>
Oxonol dye NK3630 (available from Nippon Kankoh-Shikiso Kenkyusho or Charkit Chemical Corporation)

Equipment

Heating block
Holding chamber (with capacity ≥500 mL)
Imaging apparatus (see Step 8)
Magnetic stir bar
NeuroPlex (developed by Avrum Cohen and Chun Bleau of RedShirtImaging)
Perfusion chamber
Staining chamber
Tygon tubing
Vibratome stage (e.g., 752M Vibroslice, Campden Instruments Ltd.)

Adapted from *Imaging in Neuroscience: A Laboratory Manual* (ed. Helmchen and Konnerth). CSHL Press, Cold Spring Harbor, NY, USA, 2011.

© 2015 Cold Spring Harbor Laboratory Press
Cite this protocol as *Cold Spring Harb Protoc*; doi:10.1101/pdb.prot089342

Downloaded from http://cshprotocols.cshlp.org/ at Yale University on November 6, 2015 - Published by
Cold Spring Harbor Laboratory Press

METHOD

Slice Preparation

For imaging population events, local circuits need to be well preserved with a large portion of viable neurons and functional synapses. Thin slices usually have a poor signal-to-noise ratio, owing to the smaller number of cells and to larger relative cell damage. We prefer slices with a thickness of 400–600 µm. Brain slices can be cut in several directions to conserve different aspects of cortical circuitry. Oblique directions can preserve the thalamocortical connections (Agmon and Connors 1992; Metherate and Cruikshank 1999; MacLean et al. 2006). Slices cut tangentially can best preserve the horizontal connections in layers 2/3 to observe two-dimensional waves such as spirals (Huang et al. 2004).

1. Harvest the whole brain carefully and chill in cold (0°C–4°C) modified ACSF for 90 sec.
2. Block the brain and slice it on a vibratome stage.
3. Place the brain slices into a holding chamber that contains holding ACSF. Use a chamber with a large volume (500 mL) of ACSF to help preserve local circuits.
4. Bubble the holding solution with a mixture of 95% O_2 and 5% CO_2, and slowly circulate it with a magnetic stir bar.

   Slices can be kept viable in this setting for 8–12 h. Stirring provides a slow but steady convection around the slice for delivering oxygen and washing out noxious molecules produced by the cold shock and the trauma of slicing.

Dye Staining

Absorption signals are larger than fluorescent signals in brain slices, as predicted and measured (Cohen and Lesher 1986; Jin et al. 2002).

5. Prepare the staining chamber containing ~50 mL of holding ACSF, bubbled slowly with a mixture of 95% O_2 and 5% CO_2 (about 1 bubble/sec) and circulated by a magnetic stir bar.

   Dyes have a tendency to be concentrated on the air–water interface, and slower bubbling with large bubbles can reduce the depletion of the dye from the solution.

6. Add the oxonol dye NK3630 (first synthesized by R. Hildesheim and A. Grinvald as RH482; see Momose-Sato et al. 1995 for molecular structure) and stain the brain slices.

   In the example described in Figure 1, the slices were stained with 5–20 µg/mL of NK3630. We prefer a lower dye concentration and longer staining time (1–2 h) because it results in more even staining through the thickness of the tissue.

Imaging

7. Mount the stained brain slice in a perfusion chamber on a microscope stage. Set the slice on a mesh in the center of the chamber such that both sides of the slice are well perfused. Before beginning perfusion, warm the holding ACSF by flowing it through a 100-cm section of fine Tygon tubing wound on a temperature-controlled heating block. Heat the solution slowly from room temperature to 28°C–32°C while it flows through the tubing. Perfuse with high flow rate (3–6 mL/min) and on both sides of the slice to maintain network activities in submerged chambers (Wu et al. 2005; Hajos and Mody 2009).
8. Conduct imaging.

   The optical signal from absorption dyes in brain slices ranges from 10^{-5} to 10^{-3}. We use a photodiode array (WuTech Instruments) for imaging. The array consists of 464 individual photodiodes, each glued to an end of an optical fiber (750 µm in diameter). The optical fibers are bundled coherently into a 19-mm hexagonal aperture. Photocurrent from each diode is fed into a two-stage amplifier circuit. The output of the first-stage amplifier has a very small signal of 0.05–5 mV riding on top of a large 5-V resting light signal. The resting voltage is removed by a hardware DC (resting voltage) subtraction circuit between the first- and second-stage amplifiers. The second stage has a 100×–1000× voltage gain. As a result, the two-stage amplifier construction can extend the dynamic range to ~19 bits (Cohen and Lesher 1986; Wu and Cohen 1993). We use a 14-bit data acquisition board (Microstar Laboratories, Bellevue, WA) installed in a desktop personal computer. A sampling speed of 1000–2000 frames/sec is adequate for imaging oscillations in brain slices.

   For imaging with absorption dyes, inexpensive low-NA objectives (e.g., 5× 0.12-NA, Zeiss) and a conventional 100-W halogen–tungsten filament lamp can provide excellent results. The stained slice has a peak of absorption of ~670 nm, which stays the same after a long wash with dye-free ACSF. The light transmission at the absorption peak (670 nm) is reduced to 1/10–1/50 of that of the unstained slice.

Cold Spring Harbor Protocols
www.cshprotocols.org
CSH PROTOCOLS

 Cite this protocol as *Cold Spring Harb Protoc*; doi:10.1101/pdb.prot089342

Downloaded from http://cshprotocols.cshlp.org/ at Yale University on November 6, 2015 - Published by
Cold Spring Harbor Laboratory Press

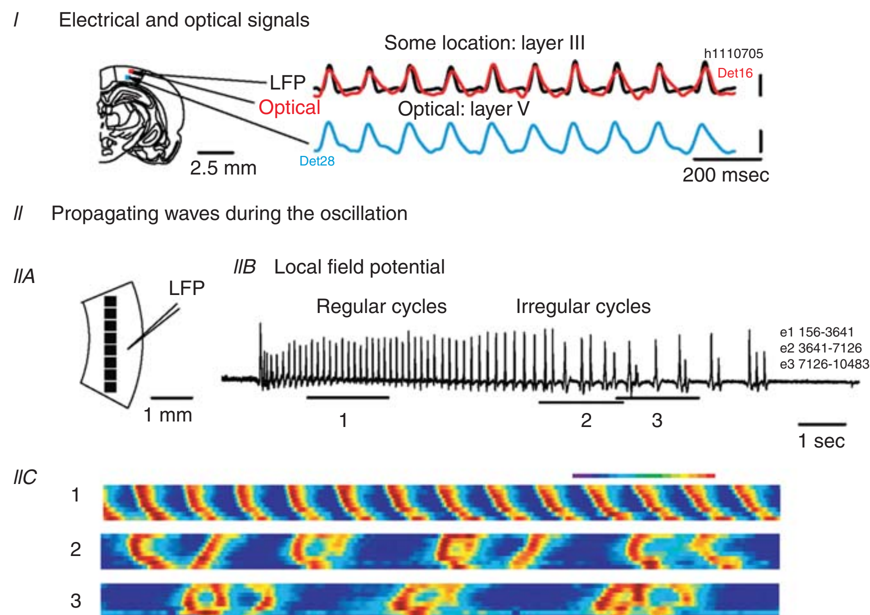

FIGURE 1. Population oscillations in a rat cortical slice. Absorption dye (an oxonol, RH482) and transillumination were used. (*I*, *left*) The recording was performed in a slice containing occipital cortex. A microelectrode recorded the local field potential (LFP) from cortical layers 2/3. Optical signals from the tissue surrounding the electrode (red square) and from layer 5 of the same column (blue square) were simultaneously recorded with the LFP. (*I*, *right*) In layers 2/3, simultaneous electrical (black) and optical (red) recordings had a similar waveform during the oscillations. In layer 5, the optical signal (blue) has the same polarity. Calibration bar, –50 µV for LFP and 10^{-4} for optical recordings. (Reprinted, with permission, from Bao and Wu 2003.) (*IIA*) Eight optical detectors (black squares) were horizontally distributed in the deep cortical layers. Their signals were used in the images in *IIC*. A local field potential microelectrode was placed in layers 2/3. (Modified, with permission, from Bao and Wu 2003.) (*IIB*) An oscillation epoch contains regular and irregular cycles. Optical signals during the periods 1, 2, and 3 (marked under the trace) are shown in *IIC*. (*IIC*) Pseudocolor images from optical signals recorded by the eight detectors. The optical signal from each detector was normalized to the maximum on that particular detector during that particular period and normalized values were assigned to colors according to a color scale (*top right*). The *x* direction of the images is time (total time ~12 sec) and the *y* direction is space in the horizontal direction in deep cortical layers, ~2.6 mm. *IIC1* are propagating waves and *IIC2* and *IIC3* are irregular patterns. (Modified, with permission, from Bao and Wu 2003.)

The dye signal (ΔI/I) and signal-to-noise ratio are maximal at 705 nm. The signal decreases below 690 nm and reaches a 0 at ~675 nm. The signal polarity reverses at wavelengths shorter than 670 nm (Jin et al. 2002). The signal reaches a second maximum at 660 nm. For nonratiometric measurement, band-pass filtering around 705 nm should yield the largest signal; an alternating illumination of 700 and 660 nm may be used for ratiometric measurements. Illumination at 675 nm results in a minimum voltage-sensitive dye signal that can be used for distinguishing dye signals from broadband intrinsic signals. The bandwidth of the filter depends on other factors: When the signal is small and shot noise is a limiting factor, a wider band pass (e.g., 715 ± 30 nm) allows more light and thus increases the signal-to-noise ratio. When measuring large signals and when long total recording time is needed, a narrower band filter of 705 ± 15 can be used for reducing dye bleaching. The heat filter (infrared filter) in the incident light path should be removed.

9. Acquire and analyze imaging data using NeuroPlex.

NeuroPlex can display the data in the form of traces for numerical analysis and pseudocolor images for studying the spatiotemporal patterns. Figure 1 shows examples of data display in which signal from the local field potential (LFP) electrode and that of an optical detector viewing the same location are plotted together. The spatiotemporal patterns of the activity are often presented with pseudocolor maps, where the signals from each individual detector are normalized to their own maximum amplitude.

DISCUSSION

The sensitivity of absorption measurements in a slice can be similar to that of local field potential measurements from the same preparation (Fig. 1) (Jin et al. 2002). Imaging with high sensitivity is important not only for detecting small population activity signals but also for detecting spatio-

Cold Spring Harbor Protocols
www.cshprotocols.org
CSH PROTOCOLS

Downloaded from http://cshprotocols.cshlp.org/ at Yale University on November 6, 2015 - Published by
Cold Spring Harbor Laboratory Press

temporal patterns without averaging across trials. Phototoxicity or photodynamic damage (Cohen and Salzberg 1978) in cortical slices appears to be irreversible even after a long dark recovery period. Absorption dyes have much less phototoxicity than the fluorescent dye RH795 in brain slice experiments (Jin et al. 2002). Intermittent light exposure also significantly reduces phototoxicity. With the same intensity (10^{12} photons/msec per mm^2), the phototoxicity using NK3630 became less significant when the exposure was broken into 2-min sessions with 2-min dark intervals; the LFP signals decreased <30% after 60 min of total exposure time. Optical signals, however, decreased ~90%. We refer to the reduction in optical signal while LFP signals remain unchanged as "bleaching." After a long light exposure, bleaching is visible even by eye as loss of color in the exposed area. Optical signals cannot be recovered in the bleached area even if the preparation is restained.

In the example shown in Figure 1, oscillations induced by carbachol were manifested as propagating waves. Each oscillation cycle was associated with one propagating wave (Fig. 1, IIC, image 1). This one-cycle one-wave pattern was seen during all oscillation cycles. Some cycles are "irregular," with the initiation site of the wave and the propagating velocity varying from cycle to cycle (Fig. 1, IIC, images 2 and 3). Complex patterns, such as collision and reflection of the waves, were also observed. In one of the cycles, the wave was apparently reflected at the edge of the tissue and the reflected waves propagated back and collided in the center, forming an "O" pattern (Fig. 1, IIC, image 3).

Cold Spring Harbor Protocols
www.cshprotocols.org
CSH PROTOCOLS

RELATED INFORMATION

To visualize spatiotemporal patterns in rodent neocortex in vivo, see **In Vivo Voltage-Sensitive Dye Imaging of Mammalian Cortex Using "Blue" Dyes** (Baker et al. 2015).

RECIPES

Holding Artificial Cerebrospinal Fluid (ACSF)

Reagent	Final concentration
NaCl	126 mM
KCl	2.5 mM
$CaCl_2$	2 mM
$MgSO_4$	2 mM
NaH_2PO_4	1.25 mM
$NaHCO_3$	26 mM
Dextrose	10 mM

Modified Artificial Cerebrospinal Fluid (ACSF)

Reagent	Final concentration
Sucrose	250 mM
KCl	3 mM
$CaCl_2$	2 mM
$MgSO_4$	2 mM
NaH_2PO_4	1.25 mM
$NaHCO_3$	27 mM
Dextrose	10 mM

Saturate the solution with 95% O_2 and 5% CO_2.

 Cite this protocol as *Cold Spring Harb Protoc*; doi:10.1101/pdb.prot089342

Downloaded from http://cshprotocols.cshlp.org/ at Yale University on November 6, 2015 - Published by Cold Spring Harbor Laboratory Press

REFERENCES

Agmon A, Connors BW. 1992. Correlation between intrinsic firing patterns and thalamocortical synaptic responses of neurons in mouse barrel cortex. *J Neurosci* **12:** 319–329.

Baker B, Gao X, Wolff BS, Jin L, Cohen LB, Bleau CX, Wu J-Y. 2015. In vivo voltage-sensitive dye imaging of mammalian cortex using "blue" dyes. *Cold Spring Harb Protoc* doi: 10.1101/pdb.prot089359.

Bao W, Wu J-Y. 2003. Propagating wave and irregular dynamics: Spatiotemporal patterns of cholinergic theta oscillations in neocortex in vitro. *J Neurophysiol* **90:** 333–341.

Cohen LB, Lesher S. 1986. Optical monitoring of membrane potential: Methods of multisite optical measurement. *Soc Gen Physiol Ser* **40:** 71–99.

Cohen LB, Salzberg BM. 1978. Optical measurement of membrane potential. *Rev Physiol Biochem Pharmacol* **83:** 35–88.

Hajos N, Mody I. 2009. Establishing a physiological environment for visualized in vitro brain slice recordings by increasing oxygen supply and modifying aCSF content. *J Neurosci Methods* **183:** 107–113.

Huang X, Troy WC, Yang Q, Ma H, Laing CR, Schiff SJ, Wu J-Y. 2004. Spiral waves in disinhibited mammalian neocortex. *J Neurosci* **24:** 9897–9902.

Jin WJ, Zhang RJ, Wu JY. 2002. Voltage-sensitive dye imaging of population neuronal activity in cortical tissue. *J Neurosci Methods* **115:** 13–27.

MacLean JN, Fenstermaker V, Watson BO, Yuste R. 2006. A visual thalamocortical slice. *Nat Methods* **3:** 129–134.

Metherate R, Cruikshank SJ. 1999. Thalamocortical inputs trigger a propagating envelope of γ-band activity in auditory cortex in vitro. *Exp Brain Res Experimentelle Hirnforschung* **126:** 160–174.

Momose-Sato Y, Sato K, Sakai T, Hirota A, Matsutani K, Kamino K. 1995. Evaluation of optimal voltage-sensitive dyes for optical monitoring of embryonic neural activity. *J Membr Biol* **144:** 167–176.

Wu J-Y, Cohen LB. 1993. Fast multisite optical measurement of membrane potential. In *Fluorescent probes for biological activity* (ed. Mason WT), pp. 389–404. Academic, New York.

Wu C, Luk WP, Gillis J, Skinner F, Zhang L. 2005. Size does matter: Generation of intrinsic network rhythms in thick mouse hippocampal slices. *J Neurophysiol* **93:** 2302–2317.

Cold Spring Harbor Protocols
www.cshprotocols.org
CSH PROTOCOLS

Downloaded from http://cshprotocols.cshlp.org/ at Yale University on November 6, 2015 - Published by
Cold Spring Harbor Laboratory Press

Cold Spring Harbor Protocols

Voltage-Sensitive Dye Imaging of Population Signals in Brain Slices

Bradley Baker, Xin Gao, Brian S. Wolff, Lei Jin, Lawrence B. Cohen, Chun X. Bleau and J.-Y. Wu

Cold Spring Harb Protoc; doi: 10.1101/pdb.prot089342

Email Alerting Service Receive free email alerts when new articles cite this article - **click here.**

Subject Categories Browse articles on similar topics from *Cold Spring Harbor Protocols.*

Imaging for Neuroscience (291 articles)
Labeling for Imaging (314 articles)
Neuroscience, general (271 articles)

To subscribe to *Cold Spring Harbor Protocols* go to:
http://cshprotocols.cshlp.org/subscriptions

© 2015 Cold Spring Harbor Laboratory Press